STUDY ON MICROSTRUCTURAL PROPERTIES OF ALUMINIUM ALLOY STRIPS FABRICATED BY LARGE STRAIN EXTRUSION MACHINING (LSEM) PROCESS

A dissertation submitted in partial fulfillment of requirement for the award of degree of

Master of Engineering

in

Production Engineering

Submitted by

KUNAL ARORA

Roll No.: 801585016

Under the guidance of

Dr. VINOD KUMAR SINGLA

Associate Professor

DEPARTMENT OF MECHANICAL ENGINEERING

THAPAR UNIVERSITY

PATIALA (PB), INDIA, 147004

JULY, 2017

Certificate

I hereby declare that the work done in this thesis entitled "**Study on Microstructural Properties of Aluminium Alloy Strips Fabricated By Large Strain Extrusion Machining (LSEM) Process**" submitted towards partial fulfillment of requirement for award of degree of **Master of Engineering** in **Production Engineering, Thapar University, Patiala,** is an authentic record of the work carried out by me under the supervision and guidance of **Dr. Vinod Kumar Singla, Associate Professor, Mechanical Engineering Department, Thapar University, Patiala.**

The matter embodied in this report has not been submitted in part or full to any other university or institute for the award of any degree.

Dated: 17/07/2017

Kunal Arora

Registration No.: 801585016

This is to certify that above declaration made by the student concerned is correct to the best of our knowledge and belief.

.....

Dr. Vinod Kumar Singla

Associate Professor

Mechanical Engineering Department

Thapar University, Patiala

ii

Acknowledgement

I would like to express my deepest sense of gratitude and a very sincere thanks to my guide **Dr. Vinod Kumar Singla**, Associate Professor, Mechanical Engineering Department, Thapar University, Patiala for his sincere and invaluable guidance and full support which helped me in the accomplishment of this dissertation report in present form. His dynamic and diligent enthusiasm has been highly instrumental in keeping my spirits high. His flawless and forthright suggestions blended with an innate intelligent application have crowned my task with success.

I would like to thank **Dr. S.K. Mohapatra,** Head of Mechanical EngineeringDepartmentand all the faculty member and staff members of Mechanical Engineering Department, Thapar University, Patiala for their boundless support.

I am also very thankful to my friends for their support during completion of the work.

KunalArora

Registration No.: 801585016

ME (Production Engineering)

Abstract

Manufacturing of bulk nano structured are in high demand in today's industry because of recent development and application of advanced materials. Many traditional machining processes were used but none of them have been able to produce complex shapes precisely at low cost. In order to improve the mechanical and micro structural properties, Large strain extrusion machining (LSEM) is introduced. It is basically a fabrication process. It is a single step manufacturing process. It is a method of severe plastic deformation (SPD) which is used particularly for machining bulk nano structured materials. It is a low cost manufacturing technique with advantage of machining and controlling dimensions simultaneously. Different controlled dimension shapes such as foils, sheets and bars are produced with controlled geometric parameters of the deformation using this machining process. In the present work, experimental investigation and analysis of formed specimen is carried out. Response surface methodology (RSM) has been used to develop the input output relations. Feed, rake angle and speed have been considered as input parameters while shear strain, hardness and surface roughness have been considered as output parameters. Aluminuim alloy AL5052 was used as the ingot material. This alloy is widely used in aircrafts, marine, railways and some other important industries. Experiments are carried out in HMT20 lathe using fabricated tool post. Based on experiments carried out, Box-Behnken design technique has been used to develop nonlinear models. The mechanical properties of the strips produced were measured by micro hardness tester. Also, the surface roughness and surface morphology of strips were studied using surface roughness tester and scanning electron microscope (SEM).

Keywords: SPD, RSM, SEM, LSEM, Nano structured materials

.

Contents

Title **Page No.**

List of Figures

List of Tables

CHAPTER 1

INTRODUCTION

1.1 Introduction

In the present scenario lightweight alloys like magnesium, titanium and aluminium have gain rapid development in the fields of aviation, aerospace technology, defense and manufacturing industries. This is due to the fact that these light weight alloys possess high strength to weight ratio and ductility. With excellent mechanical, physical and chemical properties, nanostructure materials are widely used in various fields. The fabrication processes of nanostructure material have gained attention in the recent past. So research and development is being carried out across the globe to develop components using nanostructure materials. [1] Basically nano structured materials are those whose size varies from 100-200 nanometer in length whereas ultrafine-grained materials (UFG) possess a grain size range between 300 nanometer and less than 1 micrometer in diameter. Bulk nanostructure and ultra-fine grained (UFG) metals and alloys are of extraordinary interest because of their enhanced strength properties for structural applications [2].These novel properties are not found in conventional materials. Nanostructure materials have significant mechanical properties such as high strength, hardness, limited ductility and high super plasticity at lower temperature as compared to their coarse grain counter parts. The extraordinary attributes of nanostructure material are because of small grain. Nowadays most of the research interest has been largely focused on four different subject areas, processing and fabrication, characterization of material properties, micro structural characterization, and engineering design and development for new products and applications.

1.2 Properties of Nanomaterials

The table 1.1 depicts the mechanical, physical and chemical properties of nanostructure material. The most pronounced mechanical properties of nanostructure material are high strength, hardness, ductility and super plasticity at low temperature as compared to those of conventional coarse-grained solid materials. [3]

Table 1.1 Properties of nano materials

Mechanical Properties	Physical and Chemical Properties
High Strength	Thermal stability is high
High Hardness	Wear resistance is high
Low Ductility	Corrosion resistance is high
High Super plasticity	High electrical and magnetic properties

1.3 Different approaches to produce Nanostructure Materials

There are two broad categories of approaches to synthesize nanostructure materials. The first one is "bottom up" approach and the second one is "top down" approach.

1.3.1 Bottom Up Approach

This approach is used to synthesis material from atomic or molecular species through different reactions (mainly chemical) which helps in growing the size of precursor particles. In order to obtain nanostructures with less defects, homogeneous chemical composition and better short and long range ordering bottom up approach is better. This is due to the fact that this approach is mainly driven by the Gibbs free energy which leads to produce nanostructure and nanomaterials in the state closer to thermodynamic equilibrium.

1.3.2 Top Down Approach

This approach is also known as stepwise design. Top down approach is essentially breaking down of the system into the sub system. In this approach nanostructures are formed by miniaturization of material components followed by self-assembly process. Physical forces which are operated at nano scale are used to combine basic units into large structures during self-assembly. Imperfections produced in the surface structure are one of the biggest problems with this approach [4].Also the internal stresses are also likely to be produced in this approach which leads to defects and contaminations.

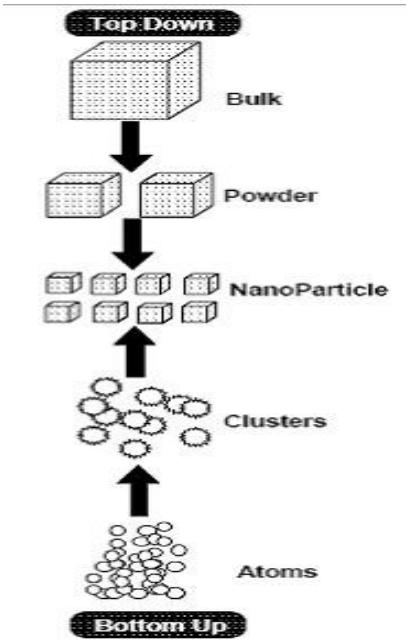

Figure 1.1 Flow diagram of both approaches [2]

1.4 Synthesizing Techniques

There are various methods of synthesizing nanostructured materials. Some of the important methods have been shown in the table below:

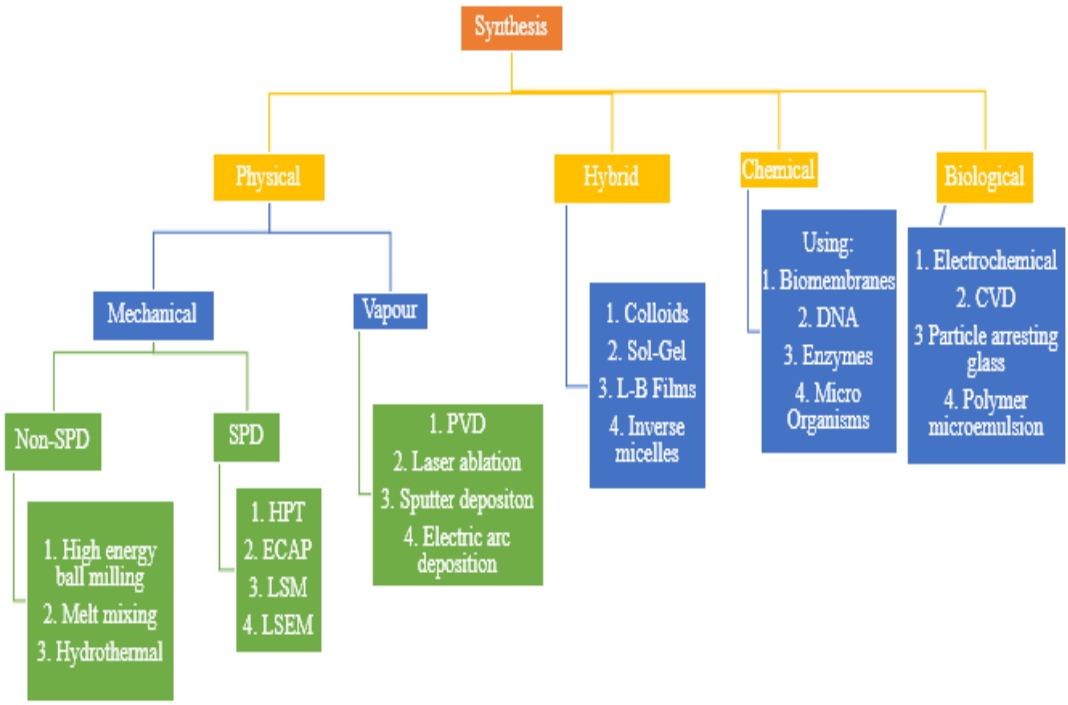

Figure 1.2 Nanostructure materials synthesizing methods [2]

1.5 SEVERE PLASTIC DEFORMATION PROCESS

Severe plastic deformation (SPD) is a metal forming process. This process is found to be most bright way to produce effective microstructure refinement. This process also produces nanostructure with enhanced mechanical properties. In SPD very large strain is applied on the bulk materials which lead to ultra-fine grained material. Different methods included in SPD are equal channel angular pressing (ECAP) and high pressure torsion (HPT) and, more recently, chip formation by machining.

1.5.1 ECAP

This process involves multiple passes of deformation to impose large plastic strains while machining is effective at imposing moderate to large strains in the chip in a single pass of deformation. In ECAP a die is constructed containing a channel that is bent through an abrupt angle equal to 90°. A sample is machined to fit in the channel and the sample is then pressed through the die using a plunger. The sample has the same cross-sectional dimensions before and after pressing, thereby permitting repetitive pressings of the same sample. It is important to note also that retaining the same cross-sectional area differentiates ECAP in a very significant way from many conventional industrial processes, such as rolling, extrusion or drawing, where the sample dimensions are reduced in each consecutive pass.

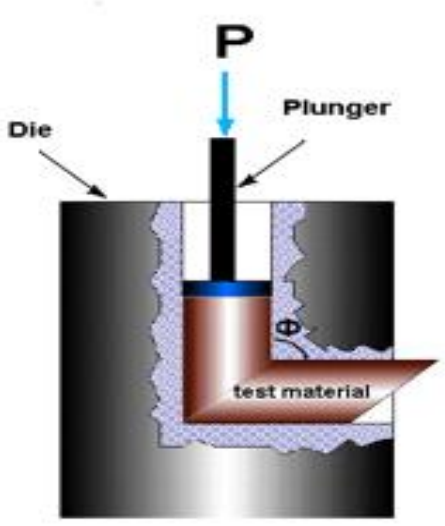

Figure 1.3 ECAP process [6]

1.5.2 HPT

The high pressure torsion (HPT) as depicted in figure 1.4 is explained in following way. The samples processed under HPT as are disc-shaped, in this process, the sample is placed between anvils and strained in torsion under an applied pressure (P) in (GPa) .The lower anvil turns and friction forces lead to a shear straining of the sample. Under high pressure, the deforming sample does not break even at high strains. To produce a homogeneous nanostructure, with a typical grain size of about 100 nm or less, deformation by several turns is necessary. [6]

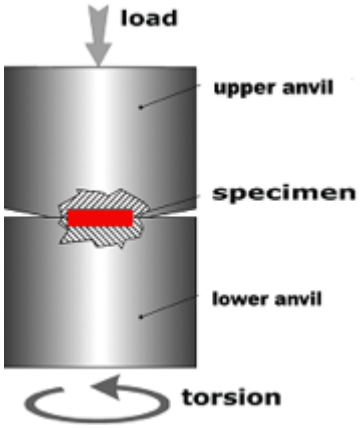

Figure 1.4 HPT process [6]

Limitations of HPT and ECAP

1. In order to create large plastic strain multiple stages of deformation are required.
2. It is found to be difficult to deform metals and alloys of high strength due to different constraints applied by operating tools.
3. Preheating is mostly mandatory at elevated temperatures.
4. The tools and equipment are very costly.

1.6 Introduction of Large Strain Extrusion Machining

Large strain extrusion machining which is a constrained machining process has been recently developed to minimize lack of control (geometric) during formation of strips. This process is basically used for producing nanostructure materials. LSEM is continuous process which includes combination of refinement in microstructure through SPD by machining and simultaneously controlling shape and dimension through extrusion. Both of these processes are done in single step. Ultra-fine grained strips of various cross sectional geometries such as

plates, bars, rods or foils are produced using LSEM. Since LSEM involves constrained chip formation, the mechanics of machining is converted into a problem of 3 constrained plastic flows akin to deformation processing (e.g. extrusion, rolling and drawing) where the exit geometry of the material is pre-defined. In the last few years of machining based deformation process has emerged as a feasible alternative to convention severe plastic deformation methods as depicted in fig 1.5. It is due to imposing large uniform plastic strain in a single pass during cutting which lead to the route of chip formation of nano structured and UFG size. Shear strains in the range 1-15 can be imposed in a variety of materials, including those of moderate to high initial strength, in a single step of deformation. But in machining, unlike conventional deformation processing methods, the geometry of the deformation and resulting chip is not determined a priori; hence, there is limited scope for control of shape and dimension of the resulting fine-grained chip material. A modification of the machining process that controls the geometry of deformation would be particularly useful for taking advantage of the simplicity of conventional machining as a method of SPD [5]. This may be realized by constraining the chip flow with a suitable "die" or "tool" placed in the vicinity of the cutting edge, thereby maintaining shear strain values on the order of those imposed by machining alone, while introducing control on the shape of the chip. Such a process would be of interest not only for the creation of bulk nano structured materials but also, for production of wire, sheet and bar with conventional microstructures, as an alternative to deformation processes such as rolling ,drawing or extrusion.

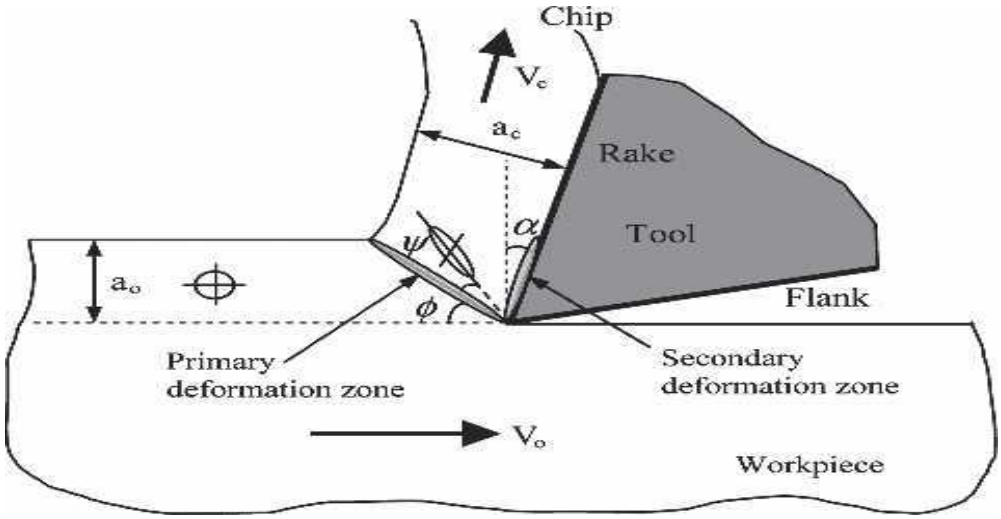

Figure 1.5 Schematic diagram of 2-D plain strain machine [7]

A method designed for this purpose, as depicted in figure, which will be called as Large strain extrusion machining (LSEM),a variant of the machining based deformation process

which combines microstructure refinement by “large-strain machining”, with shape and dimensional control of the chip by “extrusion”, simultaneously, in a single step deformation process . LSEM is a controlled method of SPD, offering a far greater level of control over deformation parameters than conventional SPD.

1.7 Background of LSEM

Large Strain Extrusion Machining (LSEM) is a process which chips are fabricated by the combination of “machining” which is done for microstructure refinement and ”extrusion” for controlling shapes and dimensions. It can also be called as extrusion-machining process. LSEM can fabricate materials in form of strips, foils, sheets, rods etc. with application of different configurations of LSEM it may be either **rotary or linear** configurations as shown in Fig. 1.6 a, b. The linear configuration of LSEM process can be elucidated as shown in Fig. a hydraulic press of high force capacity is used to drive the work piece against the tool (M2 steel, hardened to 60 Rc, and finished by grinding), while imposing a large shear strain in the chip[7]. Deformed chip thickness values in the range 1 to 10 millimeter could be readily achieved in this configuration because of the large force capacity of presses, enabling sheet specimens to be created by samples created with different levels of strain; and of the incipient stage (transient deformation stage) of chip formation.

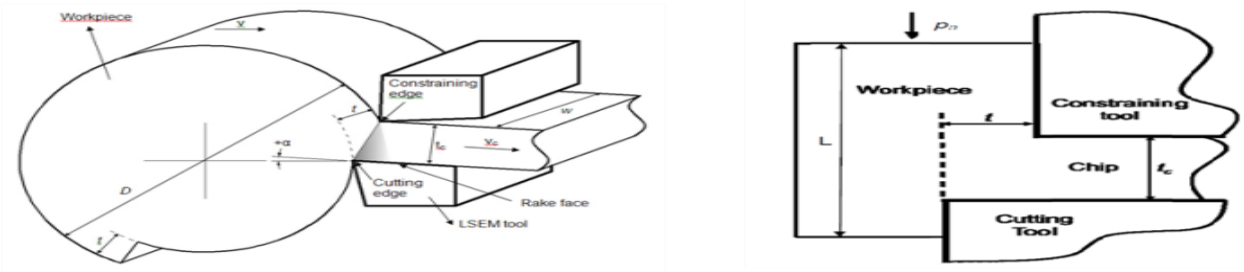

(a) (b)

Figure 1.6 Schematic of Large strain extrusion machining in (a) rotary configuration and (b) linear configuration [7]

To produce bulk nano structured (chips) of controlled dimensions in single step of deformation by especially designed tool in rotatory LSEM configuration can be elucidated herein. The LSEM tool moves radially into a disk-shaped work piece rotating at a constant peripheral speed, V. The tool consists of two components – a wedge-shaped bottom section with a sharp cutting edge inclined at a rake angle (α); and a wedge-shaped top section that

acts as a constraining edge. Both sections are made of a hard material. The machined material is simultaneously forced through an "extrusion" die formed by the bottom rake face and the top constraining edge, thereby, effecting dimensional control. Undeformed material is continuously fed into the machining zone by advancing the LSEM tool radially into the work piece at a constant feed rate of t (mm/rev). This feed is the rate of radial advance of the tool per revolution of the work piece and is the analog of the undeformed chip thickness in machining. Deformation takes place when the tool advances in the shaded region shown in Fig. 1.7. When plane strain conditions prevail, the velocity of the material at the exit of the LSEM tool is given by equation which will be covered next section of mechanics of LSEM.

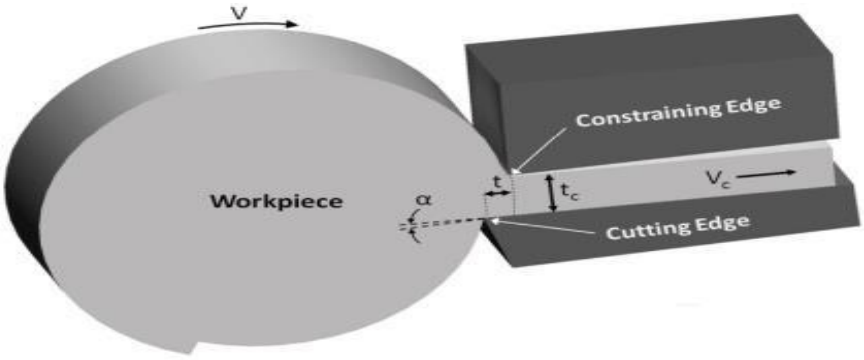

Figure 1.7 Schematic representation of LSEM [7]

1.8 Mathematical equation used in LSEM

The shear strain that is applied on plane strain LSEM due to the combination of machining and extrusion rely directly on the chip thickness ratio (λ) and the rake angle (α). Various mathematical relations of metal cutting process used to calculate chip thickness ratio (λ), shear strain (γ) and other parameters are described as follows:

$$Chip\ reduction\ coefficient, \lambda = \frac{Deformed\ chip\ thickness, tc}{Undeformed\ chip\ thickness, t}$$

$$Shear\ strain = \frac{\lambda}{cos\acute{\alpha}} + \frac{1}{\lambda cos\acute{\alpha}} - 2tan\acute{\alpha} \quad (1.1)$$

CHAPTER 2

LITERATURE SURVEY

The objective of literature survey is as following:

1. To determine the effect of various process parameters such as rake on mechanical properties of parts produced by large strain extrusion machining.
2. To minimize the drawbacks of various other process as compared to LSEM.

2.1 Classification of literature review on the basis of work material used

2.1.1 BRASS

[8]L. De Chiffre (1982) discussed a new process of cutting chips from bulk and then extruding it through the gap between the constraining tool (shoe) and cutting tool. Due to this process, continuous chips with increased ductility, hardness and luster on both the faces were produced. Some of the conditions observed during experimentation in order to carry a stable process were:

1. Shoe and cutting tool edge should be sharp so that material does not collect on the cutting tool and shoe.
2. Shoe entrance angle should be 2°.
3. Feed at the start of the process should be equal to one half of gap between shoe and cutting tool and then followed by rapid increase to full feed.

Investigation was carried out and it was found that best quality chips were produced within a speed range of 60–100 m/min at s/h= 1.5, where s was gap between the shoe & cutting tool and h was distance between shoe & edge of cutting tool. Within the above stated speed range, forces were observed to be constant which is also a favorable condition for a stable process.

2.1.2 COPPER

[9]Wen Jun Deng et al. (2012) adopted Finite Element Method (FEM) to conduct experiments on pure copper to analyze advancement of temperature field, effective strain, and strain rate at distinct chip compression ratios. The cutting and thrust forces were also analyzed with respect to time. As the value of chip compression ratio (λ) decreased, nano grained material formation was facilitated due to increases in effective strain. But at t0he same instant, thrust & cutting forces also increased with time at the particular values of λ and it became difficult to push the chips of the deformation zone. Results concluded from the study assured a steady LSEM process.

[10]Wen Jun Deng et al. (2013) adopted Finite Element Method (FEM) (DEFORM-2D software) to investigate and analyze the effect of constraining tool corner radius(R) on deformation behavior of pure copper and studies were conducted on structure refinement of chips in LSEM. The effective strains and strain rates distribution were very sensitive to the constraining tool corner radius because the change in tool corner radius affects the friction at the tool chip interface which further significantly affects the effective strain related with chip formation and hence the chip morphology. With increase in tool corner radius, a significant increase in effective strain was observed with simultaneous decrease in strain rate. Hence a wide range of ultrafine grained materials were obtained by changing the Constraining tool corner radius.

[11]Wen Jun Deng et al. (2014) adopted Finite Element Method (FEM)(DEFORM-2D software) to investigate the influence of rake angle on large strain extrusion machining and validated it with the results when the experiment on plain strain extrusion machining were conducted physically. Simulations were done at very low speed of 0.052m/s with rake angle values varied from 5° to 30° with an increment of 5°. Continuous chip formation was observed with chips significantly much harder and grain size smaller than the bulk material. A significant increase in cutting forces was also recorded with decrease in rake angle.

[12]S.L. Cai et al. (2015) conducted experiments on special copper known as Oxygen free high conductivity (OFHC) copper using a specially designed LSEM machine. They have measured material particle flow field in strips by using high speed imaging and digital image correlation (DIC) in LSEM. They have also developed new form of mathematical model in order to replicate the results of the process. It observed that the constraining tool makes the materials moving into the shear plane to deviate from its original path by an

angle (β). The angle (β) increases as the chip thickness ratio decreases. A new equation for shear strain was developed as follows:-

$$\gamma = \frac{\lambda - sin\beta + cos\alpha tan\beta}{cos\alpha - (\lambda - sin\alpha)tan\beta} + \frac{1}{\lambda cos\alpha} - tan\alpha \qquad (2.1)$$

The maximum difference between the calculated and the observed values of chip thickness ratio and strain were about 13% and 6% respectively and were due to the tolerance of the proposed experimental setup.

Table 2.1Chemical composition of OFHC copper [12]

Elements	Cu+Ag	Fe	S	Pb	Zn	Sn	O	Others
Wt(%)	99.97	0.004	0.004	0.003	0.003	0.002	0.002	0.001

[13]W. Moscoso et al. (2007) adopted LSEM and performed a series of experiments in order to study the enhanced characteristics of nanostructured materials and ultra-fine grains (UFG) created in the form of foil, sheets, wires, rods, plates by using single pass deformation. Data obtained from experimentation using different level of strains imposed on bulk material of OFHC copper illustrated that the hardness of nanostructured chips were significantly higher than the bulk material. By doing TEM analysis it was found that as we increase strain there was evolution of refinement of microstructure and formation of ultra-fine grain structure. At lower value of strain, elongated UFG microstructure were observed, while at moderate values equi-axed UFG was seen, and lastly, at highest strain, UFG of average grain diameter 250 nm was revealed.

[14]P.lin et al.(2013) have analyzed the effect of coefficient of friction (μ) on deformation behavior in LSEM using finite element method (FEM). A series of simulations were conducted using FEM model to obtain distribution of simulated effective strain with different friction coefficients. It was observed that there was increase in level of effective rate of strain as coefficient of friction increased. It was also manifested. At higher value of μ chip faces difficulty to get pushed out and chip gets deformed more in homogeneously at this point. When cutting length was same the lengths of chip that were detached from workpiece are different at different coefficients of friction.

[15]Iglesias, et al.(2010) have analyzed the effect of wear resistance of nanostructured material of copper (Cu) fabricated by LSEM as a function of microstructure and sliding

direction of ball-on-flat configuration under variable shear strain. The lowest wear volume was obtained when the sliding takes place in the perpendicular direction to that of grain orientation. The highest wear resistance was observed for nanostructure copper material with an elongated grain structure in the extrusion direction. The wear resistance of this anisotropic material depends on the sliding direction.

[16]Brownet al. (**2009)** have observed the effects of interaction of deformation field on the microstructure of copper alloy during the machining of LSEM process. The microstructure evolution at different deformation rates led to development of following results. As we increase the strain at small deformation rates, the proportion of high angle boundary increases which leads to grain refinement in LSEM. However as the strain rate is decreased it was found that microstructure development is the single pass SPD was very similar to that found in multiple pass.

2.1.3 ALUMINIUM

[17]Andrew Kustas et al. (2014) employed LSEM to study its practicability in eliminating porosity from a casted ingot of aluminum 5052 acquired from hydrogen entrapment during melting & casting and volumetric shrinkage during solidification. Optical microscopy of bulk and fabricated strips was performed to compare porosity level, which was followed by Limiting Dome Height (LDH) test to compare the mechanical properties of strips produced from LSEM and conventional rolling. Optical micrographs, of the strip indicated significant porosity reduction, due to high shear strain and hydrostatic pressure during extrusion. Mechanical behavior of LSEM strips from LDH test was discovered to be ranging within conventionally rolled and annealed strips.

[18]M Ravi Shankar et al. (2005) investigated and highlighted the mechanical properties of precipitate treatable tempered alloys of aluminium. Growth of microstructure of chips in deformation zone was observed. The microstructure study suggested chips consists of equiaxed grains nearly of mean size of grains 70-100nm. The chip micro-hardness values suggested they were found to be somewhat greater than that obtained from ECAP deformation for Al6061-T6 alloy.

[19]W.J. Deng et al. (2014) studied the thermal stability of ultra-fine grains of Al alloy fabricated by LSEM. Aluminum alloy strips were heat treated via annealing process in order to study thermal effects on their microstructure and mechanical properties. A set of different temperatures and different length of time were used to perform annealing process.

Ultra-fine grains of Al alloy chips can maintain high hardness under 200°C but start losing hardness as temperature increases to 300°C and above. It was found that when the temperature is less than 200°C during annealing most of the fine grains were transformed to elongated grain. The grain size of these elongated grains increased in aspect ratio as the annealing time increases. However Vickers hardness was almost same as was expected due to precipitation of second phases.

2.1.4 MAGNESIUM

[20]Mert et al.(2007)analyzed the mechanics of LSEM in which high deformation rate and high hydrostatic pressure have been applied in a single step on Magnesium alloy (MgAZ31B) for the continuous production of Mg alloys in bulk form to sheets and foil. Hydrostatic pressure and temperature in the deformation zone were found to be function of chip thickness ratio, rake angle. Capabilities to realize combinations of large strain, large hydrostatic pressure and low temperature levels, especially in a highly confined region (primary deformation zone), promoted the workability and grain refinement of alloys.

2.1.5 STEEL

[21]P. Iglesias et al. (2008) discussed new machining-based manufacturing processes with the use of which, nanostructured materials could be manufactured much economically as compared to existing methods to do so. Shift from LSM to LSEM has been justified on PH13-8Mo Stainless steel since LSEM is combination of refinement of microstructure via large strain machining while shape and dimension of chips are controlled by extrusion, whereas in the former method only grain refinement was possible. Further a cost analysis was made considering machining cost/hour C, cutting velocity V, exit sheet (chip) thickness of t_c, chip thickness ratio and sheet width of w. The cost per unit volume (euros/cm3) is then,

$$C_{vol} = \frac{\lambda.C}{3.6\,.w.v.tc} \qquad (2.2)$$

2.1.6 LEAD

[22]Y. Guo et al. (2012) employed LSEM to study of large-strain deformation phenomena in commercially available pure lead under high level of hydrostatic pressure is applied on the shear zone. Experimentation was done under following conditions: - rake angle (α) = 10°, uncut chip thickness (h_0) = 0.2mm, cutting velocity (v_0) = 10mm s^{-1}, and chip thickness ratio

(λ) ranging from 0.4 to 2.5. Rate of change of strain $\frac{d\varepsilon}{dt}$ attains its highest value at λ=1. Strain increases as the value of λ increases and further can be enhanced by reducing the shear angle value (α).

2.2 CONCLUSIONS FROM LITERATURE SURVEY

1. The effect of rake angle, chip thickness ratio, constraining tool radius and coefficient of friction on LSEM has been analyzed.
2. The formation mechanism of chips and machining parameters needed for nanostructure/ UFG strip formation in LSEM were discussed.

3. The result shows that rake angle and chip compression ratio have a significant impact on total shear strain for the strip.

4. The decrease in the rake angle causes effective strain and strain rate to be increased. But smaller the rake angle, the smaller in grain sizes the microstructure was obtained.

5. The decrease in chip thickness ratio will also cause effective strain and strain rate to be increased. But smaller the chip thickness ratio, the smaller in grain sizes the microstructure was obtained.

6. With the constraining tool corner radius or the friction coefficient increases, the strip effective strain, temperature, stress on the strip also increase, which can impact the microstructure and mechanical properties of the strip.

7. The hardness of nanostructure chips was significantly higher than the bulk material.

8. With increase in shear strain the evolution of microstructure refinement of UFG structures was found.

9. The wear rate analysis showcased that the wear rate of nanostructured material are less than micro structured material.

10. Creation of thick sheet from large strain extrusion machining was best achieved using high hydrostatic pressure or large deformation temperature.

11. During the thermal stability studies, it was found that UFG of Al alloy chips maintained high hardness under 200°C but started losing their hardness as temperature increases to 300°C and above .

12. When cutting length are same the length of chip detached from work piece are different for different coefficient of friction.

2.3 GAPS IN LITERATURE

1. The framework to incorporate temperature effects arising at higher speeds, and rubbing induced deformation at the cutting edge. These aspects should also be facilitated by studying of a range of alloys and its process conditions,
2. The quantitative analysis of the microstructure refinement for nanostructure material has not been studied till date.
3. The mechanics of deformation for difficult to machine materials like aluminium alloys are yet not fully explored using LSEM process.
4. Corrosion resistance studies of nanostructure chips are yet to be performed.
5. The power requirements for achieving smaller grain sizes in the thicker strips have not been fully explored till date.
6. XRD analysis is yet to be performed to study microstructure refinement studies.
7. A wide range of scope lies in heat treatment studies for produces chips.

2.4 PROBLEM FORMULATION

On the basis of literature survey discussed above, the present work aims to investigate the effect of various process parameters on the various mechanical properties of AL5052 aluminium alloy by using large strain extrusion machining process. The process parameters are feed, speed and rake angle. The responses were micro hardness and surface roughness. The entire experiment was carried out on HMT-20 lathe machine available at Machine Tool Lab, Thapar University, Patiala.

2.5 OBJECTIVES

1. Fabrication of nanostructure strips of Al5052 using LSEM under different machining conditions.

2. To study the effect of machining parameters on shear strain induced in chips during LSEM.

3.To investigate the effect of process parameters on mechanical properties of final product.

4. To investigate the significant interaction between the above factors.

5. To study the microstructure analysis of machined surface.

These objectives have been completed by using Box-Behnken design technique and scanning electron microscope (SEM).

CHAPTER 3

DESIGN OF EXPERIMENTS

3.1 INTRODUCTION

Large strain extrusion machining (LSEM) is a single step process which includes extrusion and machining simultaneously. In this process fine quality of chips are produced. Accurate surface finish and high hardness can be achieved by using LSEM. The impact of various input parameters on responses have been studied after producing chips. The various input parameters were rake angle, feed and speed. Experiments were designed by using Design expert software. This software runs the experiments randomly. Box-Behnken design technique was used for conducting the experiment. It plays an important role for achieving the high efficiency of the response surface methodology. Box Behnken design experiments require lesser experiments as compare to Central Composite design. The proposed Box Behnken design requires 17 experiments since there are three parameters.

3.2 SELECTION OF FACTORS

Fish bone diagram was used to determine the factors which improve the quality of strips produced. It is shown in Figure 3.1.The process parameters with their different levels have been selected after exhaustive literature survey. The selected parameters are shown in Table 3.1.

Table 3.1 Selected Factors and their ranges

FACTORS	LEVEL 1	LEVEL 2	LEVEL 3
Tool Rake Angle (^{O})	-5	0	5
SPEED(m/min)	30	90	150
FEED (mm)	0.05	0.10	0.15

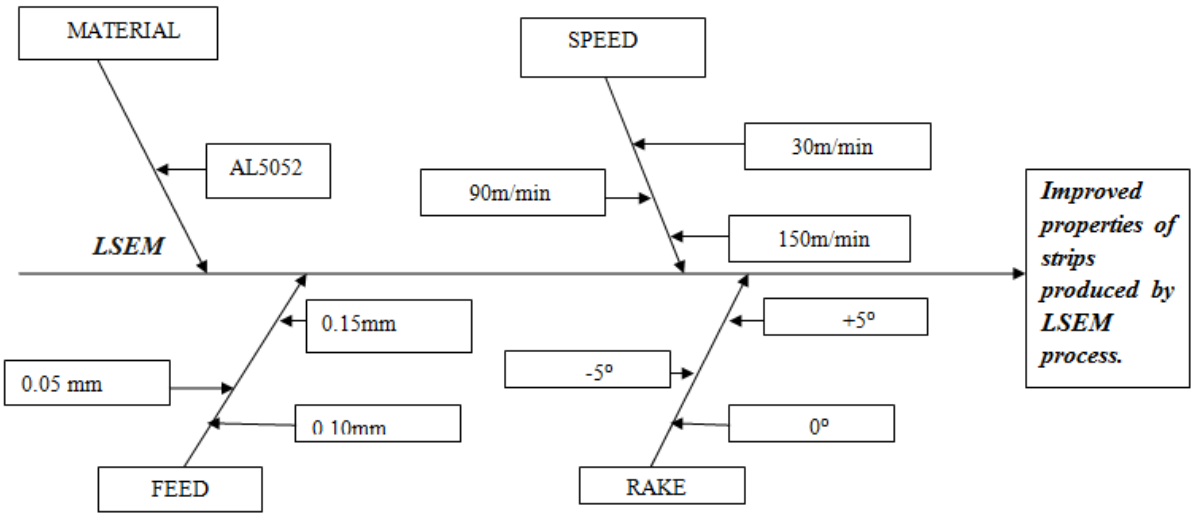

Figure 3.1 Cause and effect diagram of LSEM

3.3 BOX-BEHNKEN DESIGN

Box-behnken design technique plays an important role for achieving the high efficiency of the response surface methodology. Response surface methodology (RSM) consists of a group of statistical and mathematical technique used to optimize the output parameter which is affected by several input parameter. RSM technique is used in designing, developing and analyzing new technical studying and products. It is also an effective technique in development of existing studies and products. It is a cost effective technique.

The efficiency of Box-Behnken design is higher for an experiment involving three factors and three levels. Box Behnken design experiments require lesser experiments as compare to Central Composite design. The proposed Box Behnken design requires 17 experiments. Experiments were designed by using Design expert software. This software runs the experiments randomly. 2D and 3D plots of responses were also developed by Design expert software. Such plots clear give an idea of the influence process variable over others; further the plots present the trend of variables interaction in the process. Regression model was developed and its acceptability was validated to forecast the output values at nearly all conditions. Further the model was verified by performing experiments, taking two sets of random input values. The response values measured through experiments are similar with the predicted values using the model.

The experimental data collected as per BBD was used.

Table 3.2 Trail conditions using BBD

STD	RUN	A:Rake(°)	B:Speed(m/min)	C:Feed(mm)
10	1	0	150	0.05
12	2	0	150	0.15
6	3	5	90	0.05
4	4	5	150	0.10
1	5	-5	30	0.10
3	6	-5	150	0.10
8	7	5	90	0.15
14	8	0	90	0.10
5	9	-5	90	0.05
15	10	0	90	0.10
11	11	0	30	0.15
17	12	0	90	0.10
13	13	0	90	0.10
7	14	-5	90	0.15
16	15	0	90	0.10
9	16	0	30	0.05
2	17	5	30	0.10

3.4 EXPERIMENTAL SET UP

In the current investigation, effect of various large strain extrusion machining process parameters are studied. The process parameters are tool rake angle, feed and rpm. AL5052 aluminium alloy is used as a raw material. 2HP universal lathe with rotary configuration is used to produce the strips. Special design tools made of HSS were used to replace conventional cutting tool. Special designed tool post was also prepared. The machining is done radially at different speeds and feed. Machining was done without using lubricant. With continuous feeding of tool, strips of different lengths were extruded from the tool. Experiments were conducted as per Box-Behnken Design (BBD) with the help of design of expert (DOE).The entire experiments were carried out in Advance Machining Lab, Thapar University Patiala.

Table 3.3 AL5052 COMPOSITION

ALUMINIM	MAGNESIUM	CHROMIUM	COPPER	IRON	MANGANESE	ZINC	SILICON	OTHERS
97%	2.2%	0.15%	0.1%	0.4%	0.1%	0.1%	0.25%	0.20

3.4.1 Tool post and tools used for experiment

A special design cutting tools and tool post were used. Tool post made of mild steel has been fabricated. Similarly special cutting tools made of HSS were made of angles 0°, 5° and -5° respectively. One constraint tool was also made. All these tools were heat treated. Cylindrical rod of AL5052 was used of diameter 6cm and length 20cm as a work piece.

(a)+ 5^0 rake angle cutting tool

(b)-5^0 rake angle cutting tool

(c) Constraining tool

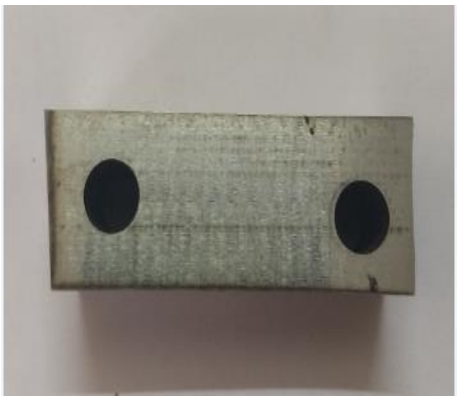

(d) 0^0 rake angle cutting tool

Figure 3.2 Tool of different rake angles

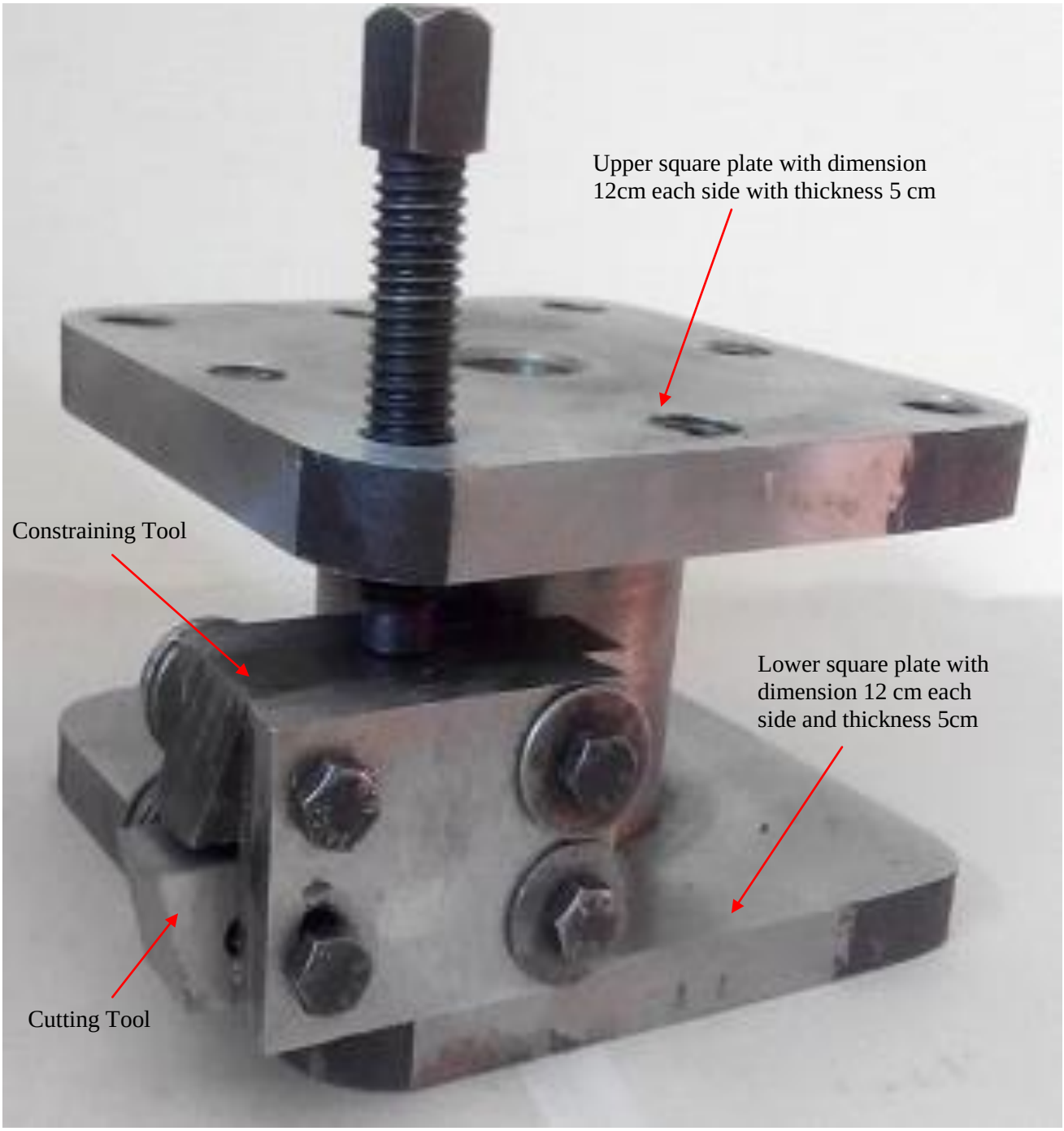

Figure 3.3 Fabricated tool post

(a) Strip at 0^0,30m/min,0.05mm feed

(b)Strip at+ 5^0,30m/min,0.05mm feed

(c) Strip at -5^0,30m/min,0.05mm feed

(d) Strip at 0^0,90m/min,0.10mm feed

(e) Strip at +5^0, 90m/min, 0.10mm feed

(f) Strip at -5^0,90m/min,0.10mm feed

Figure 3.4 Strips at different rake angles

3.5 EQUIPMENTS USED

Micro Hardness and Surface Roughness test were performed on all the strips. For surface morphology Scanning Electron Microscope(SEM) was used. The test equipments used for measurement of these responses are given below:

3.5.1 Micro hardness test

Micro hardness analysis was done to measure the penetration resistance of the specimen. Measurements were done on a computer Interfaced Micro Hardness Tester (Model: MVH2), available at Thapar University, Patiala. The micro hardness measurement is dependent on the diameter of indentation produced on the samples. Indentation was done with a diamond cone indenter at a constant load of 100 gm/mm^2 for a dwell period of 20 sec with Quantimet software. 40 MP cameras were used for observing / focusing images.

Figure 3.5 Micro hardness testing machine (Model: MVH2)
(Courtsey: Measurement and Control Lab,Thapar University)

3.5.2 Surface Roughness Tester

Surface roughness was measured using the Mitutoyo model SJ-400, Germany. The equipment uses the stylus method of measurement, has profile resolution of 12 nm and measures roughness up to 100 μm. A tracing length of 4.8 mm was used for analysis. Surface Roughness values were taken two times for each trial and average was used for analysis.

Figure 3.6 Surface roughness tester (Model SJ400)
(Courtsey:Metrology Lab,ThaparUniversity,Patiala)

3.5.3 X-RAY Diffraction

XRD analysis was performed using Panalytical X-Pert Pro diffractometer (θ - 2θ) equipped with Cu-Kα radiation (λ = 1.5418 Å). The specimens for X-ray diffraction examination were prepared by grinding with SiC papers of up to 2000 grit size to flat grounded surfaces for performing 2-theta scanning of all samples for quantitative analysis of deformation behavior at different process conditions.

Figure 3.7 X-RAY Diffraction

(Courtsey: SAI Lab, Thapar University, Patiala)

3.5.4 Scanning Electron Microscope

The surface morphology of chips produced by LSEM has been investigated by scanning electron microscope model JSM-6510LV. The scanning electron microscope is a type of electron microscope that produces images of a sample by scanning it with a high energy beam of electrons. The SEM images were taken at 500x and 1000x resolution. The effect of feed and speed on surface quality of AL5052 chips produced by different rake angles.

Figure 3.8 Scanning Electron Microscope

(Courtsey: SAI Lab, Thapar University, Patiala)

3.6 ANALYSIS OF RESULTS

The experimental data collected as per BBD was used.

The result of Micro Hardness and Surface Roughness for AL5052 is shown in Table 3.4

Table 3.4 Experimental obtained values of Micro Hardness and Surface roughness of AL5052

STD	RUN	A:Rake(°)	B:Speed (m/min)	C:Feed(mm)	RESPONSE: Microhardness(HV)	Response: Surface Roughness(μm)
10	1	0	150	0.05	100.62	2.53
12	2	0	150	0.15	101.2	2.60
6	3	5	90	0.05	101.26	1.62
4	4	5	150	0.10	96	1.38
1	5	-5	30	0.10	148.06	1.32
3	6	-5	150	0.10	96.32	1.35
8	7	5	90	0.15	102.32	1.61
14	8	0	90	0.10	107.76	2.65
5	9	-5	90	0.05	111.52	1.5
15	10	0	90	0.10	108.76	2.72

11	11	0	30	0.15	148.02	2.95
17	12	0	90	0.10	110.79	2.68
13	13	0	90	0.10	108.79	2.62
7	14	-5	90	0.15	112.32	1.2
16	15	0	90	0.10	112.38	2.78
9	16	0	30	0.05	148.23	2.86
2	17	5	30	0.10	141.32	1.72

3.7 RESPONSE CHARACTERISTICS

Response Characteristics of this experimental work is shown in Table 3.5. Strips produced by LSEM should have higher Micro Hardness values but lower Surface Roughness values.

Table 3.5 Response Characteristics

Response name	Response type	Units
Micro Hardness	Higher is better	HV
Surface Roughness	Lower is better	Microns

CHAPTER 4

RESULTS AND ANALYSIS

4.1 INTRODUCTION

The effect of various process parameters such as(rake angle, feed and speed) on mechanical properties such as micro hardness, surface roughness. Effect of shear strain and surface morphology was also analyzed.AL5052 Aluminium alloy cylindrical rod was used for this experimental work. Design Expert software was used for experimental work. In this proposed investigation all the three factors were varied at three levels. After conducting the 17 trials the mean value of all the factors are tabulated.

4.2 ANALYSIS OF AL5052 ALUMINIUM ALLOY

The experimental data collected as per BBD was used.

4.2.1 Results for Micro Hardness

Micro Hardness of strips was measured by Vicker hardness tester machine.

The equation developed for response hardness is given below:

$$MICROHARDNESS = 176.157 - 1.1875 \times A - 1.0819 \times B - 11.03 \times C - 0.1283 \times A \times A + 0.0038 \times B \times B + 153.9 \times C \times C + 0.0053 \times A \times B + 0.22 \times A \times C - 0.1008 \times B \times C \quad (4.1)$$

Table 4.1 ANOVA table for micro hardness

SOURCE	SUM OF SQUARES	DF	MEAN SQUARE	F-VALUE	PROB>F	Percentage Composition	STATUS
Model	5443.32	9	604.84	111.21	<0.0001		Significant
A	71.24	1	71.24	13.10	0.0085	1.67	Significant
B	3298.20	1	3298.20	606.46	<0.0001	77.48	Significant
C	0.18	1	0.18	0.033	0.8607	0.04	Not Significant
A^2	43.32	1	43.32	7.97	0.0257	1.01	Significant
B^2	818.76	1	818.76	150.55	<0.0001	19.29	Significant
C^2	0.62	1	0.62	0.11	0.7449	0.014	Not Significant
AB	10.30	1	10.30	1.89	0.2111	0.241	Not Significant
AC	0.012	1	0.012	0.002225	0.9637	0.002	Not Significant
BC	0.37	1	0.067	0.067	0.8028	0.008	Not

							Significant
Residual	38.07	7	5.44				Not Significant
Lack of fit	24.62	3	8.21	2.44	0.2043		Not Significant
Pure Error	13.45	4	3.36			0.3159	
Cor total	5481.59	16					

Significant Factor: A, B, A^2 , B^2

Insignificant factor:C, C^2, AC, BC,AB

Following things can be observed from analysis:

1. Model "F-Value" is 111.21 which imply model is significant. There is only 0.01% chance that model with this large value could occur due to noise.

2. Values of "Prob>F" lest than 0.05 indicates that model terms are significant. For given model A (Rake angle), B (Speed), A^2 (square of rake angle) and B^2(square of speed) are significant.

3. Values greater than 0.05 are totally insignificant.

4. The "Lack of Fit-F value" of 2.44 implies that Lack of Fit is not significant relative to pure error. There is 20.43% chance that "Lack of Fit-F value" this large could not occur due to noise. Non-significant lack of fit is good –We want model to be fit.

The values of R-Squared given by software are as follows

Table 4.2 ANOVA parameters

R-Squared	0.9931
Adj R-Squared	0.9841
Pred R-Squared	0.9243
Adeq Precision	30.310

- The "Pred R-Squared value" of 0.9243 is reasonable agreement with the "Adj R-Squared value" of 0.9841.
- "Adequate precision "value measure signal of noise ratio. It is desirable to have ratio greater than 4. Ratio of 30.310 indicates adequate signal. Hence model can be used.

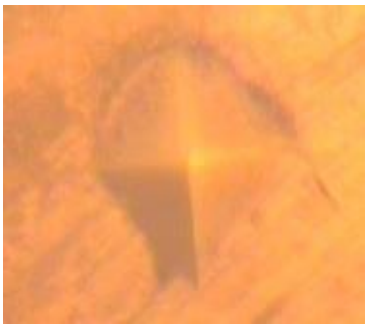

(a)Indentation at 0^0, 30m/min and 0.05mm feed

(b) Indentation at 0^0, 90m/min and 0.05mm feed

(c) Indentation at 0^0,150m/min and 0.05mm feed

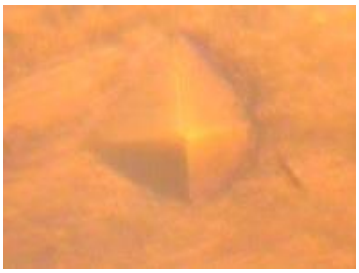

(d) Indentation at 5^0, 30m/min and 0.05mm feed

(e) Indentation at 5^0, 90m/min and 0.05mm feed

(f) Indentation at 5^0, 150m/min and 0.05mm feed

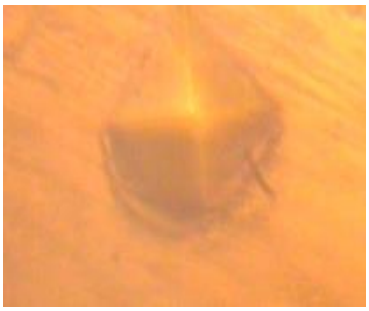

(g) Indentation at -5^0, 30m/min and 0.05mm feed

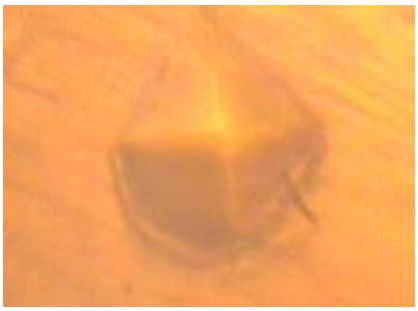

(h) Indentation at -5^0, 90m/min and 0.05mm feed

Figure 4.1 Images of indentation of trials

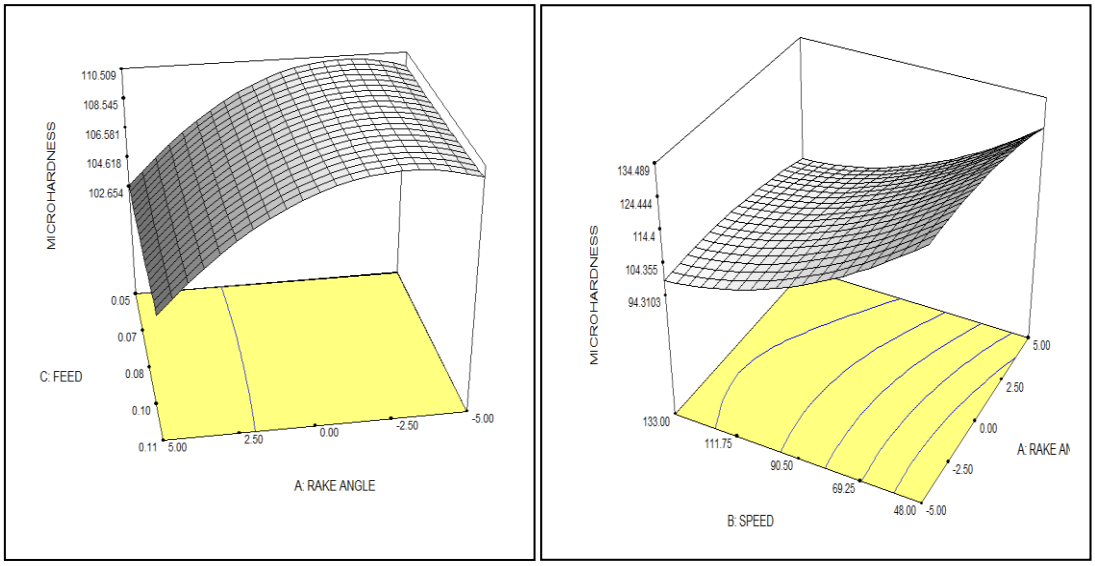

(a) (b)

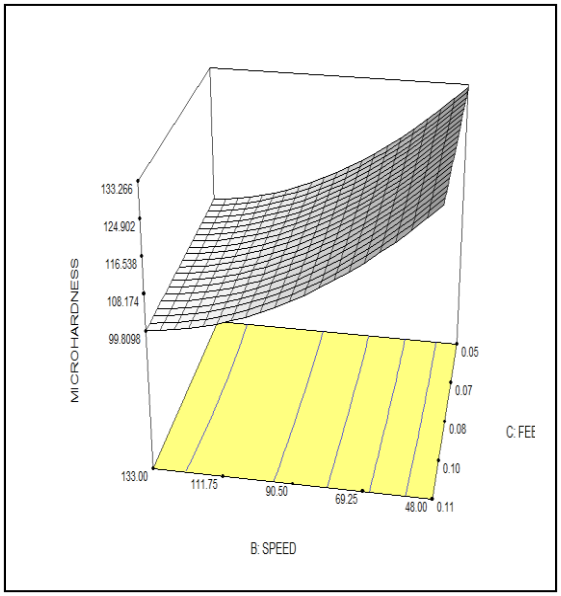

(c)

Figure 4.2 3-D plot of variation of (a) feed and rake v/s micro hardness, (b) speed and rake v/s micro hardness, (c) speed and feed v/s micro hardness

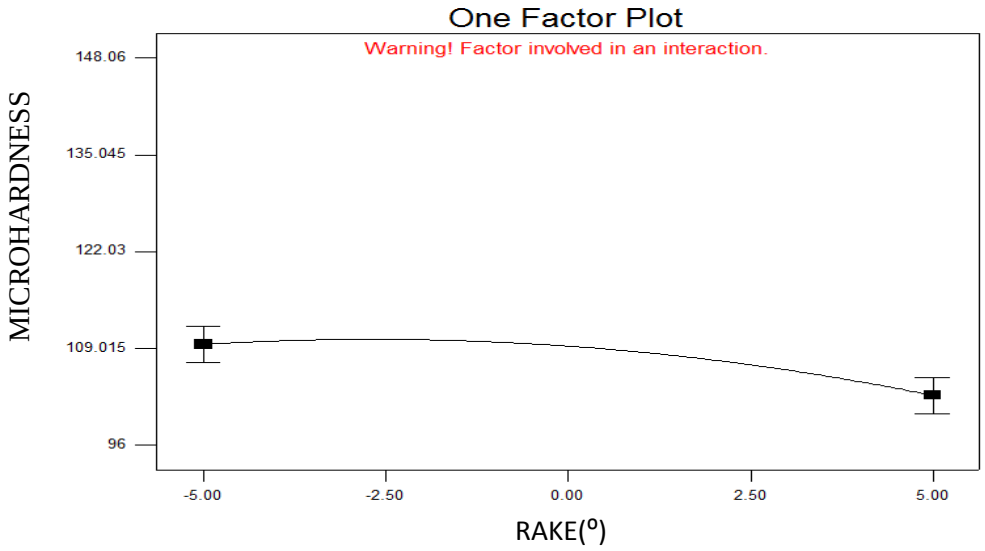

(a)

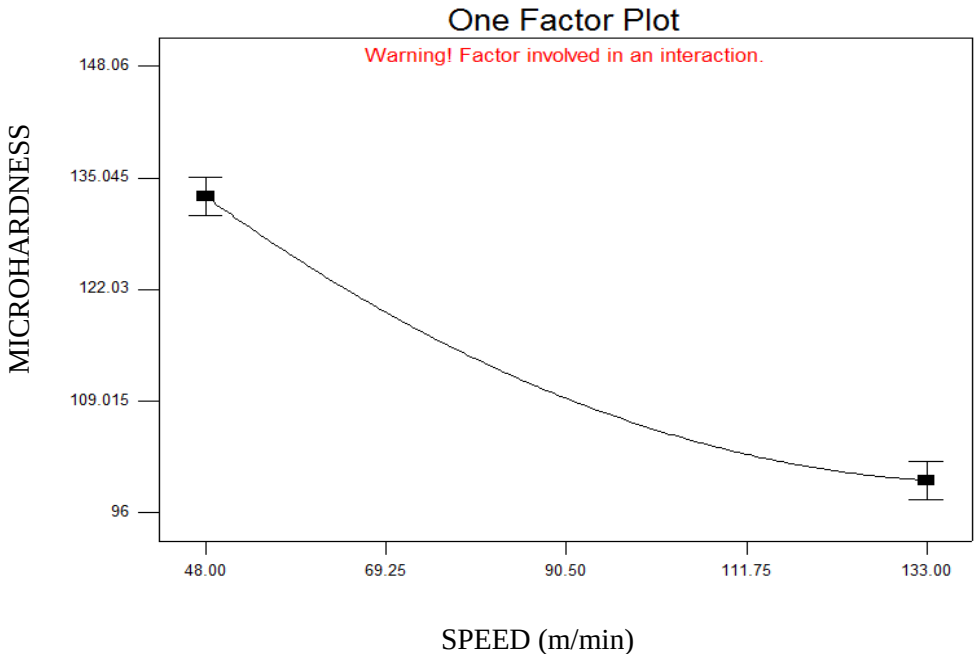

(b)

Figure 4.3 Variation of (a) Micro hardness v/s rake and (b) Micro hardness v/s speed

The effect of rake angle and speed is shown on hardness at different process parameter is shown in figure 4.3a and 4.3b respectively. The trend portrays reduction in hardness with increase in cutting speed (from 30m/min to 150m/min) and decrease in rake angle (from +5° to -5°). With decrease in rake angle, forces and stresses in the PDZ increases, causing a driving force to the dislocations piled up along the grain boundaries causes low angle grain boundaries, resulting in sub grain formation or grain refinement. This grain refinement increases the dislocation density causing increased hardness of the material. For a given rake angle, as the cutting speed increases temperature in the PDZ increases which promotes grain growth in the material, because of which the hardness of the material decreases. Dinakar Sagapuram et al have studied the effect of cutting speed on hardness and deformation temperature and a similar trend was observed in their study. [22]

4.2.2 Results for Surface Roughness

Mitutoyo model SJ-400 tester was used for measurement of surface roughness. The tester uses a stylus method of measurement. Tester has a profile resolution of 12nm and surface roughness can be measure upto 100µm. In this experiment tracing length of 4.8 mm was used.

The equation developed for response surface roughness is given below:

$$Surface\ roughness = 3.073 + 0.0228 \times A - 0.0021 \times B - 3.625 \times C - 0.05 \times A \times A + 0.00007 \times B \times B + 17 \times C \times C - 0.0003 \times A \times B + 0.29 \times A \times C - 0.0017 \times B \times C \quad (4.2)$$

Table 4.3 ANOVA table for Surface Roughness

SOURCE	SUM OF SQUARES	DF	MEAN SQUARE	F-VALUE	PROB>F	Percentage Composition	STATUS
Model	6.89	9	0.77	87.09	<0.0001		Significant
A	0.049	1	0.049	5.61	0.0497	0.70	Significant
B	0.090	1	0.090	10.20	0.0152	1.29	Significant
C	0.010	1	0.010	1.14	0.3204	0.143	Not Significant
A^2	6.58	1	6.58	747.91	<0.0001	94.64	Significant
B^2	0.0002632	1	0.0002632	0.002992	0.9579	0.03	Not Significant
C^2	0.007605	1	0.007605	0.86	0.3834	0.109	Not Significant
AB	0.034	1	0.034	3.89	0.0892	0.489	Not Significant
AC	0.021	1	0.021	2.39	0.1660	0.302	Not Significant
BC	0.0001	1	0.0001	0.011	0.9181	0.0014	Not Significant

Residual	0.062	7	0.008796				
Lack of fit	0.046	3	0.015	3.93	0.1096		Not Significant
Pure Error	0.16	4	0.0039			2.307	
Cor total	6.96	106					

***Significant Factor**:* A, B, A^2

***Insignificant factor**:*C,B^2, AB, AC, BC,C^2

In the following model we have taken interaction between A(rake), B(speed) , C (feed) , there squares A^2 , B^2 ,C^2 and also interaction between them AB , BC , CA.

Following things can be observed from analysis:

1. Model "F-Value" is 87.09 which imply model is significant. There is only 0.01% chance that model with this large value could occur due to noise.

2. Values of "Prob>F" lest than 0.05 indicates that model terms are significant. For given model A (Rake angle) , B (Speed) and A^2 (square of rake angle) are significant.

3. Values greater than 0.1 are totally insignificant.

4. The "Lack of Fit-F value" of 3.93 implies that Lack of Fit is not significant relative to pure error. There is 10.96% chance that "Lack of Fit-F value" this large could not occur due to noise. Non significant lack of fit is good –We want model to be fit.

The values of R-Squared given by software are as follows

Table 4.4 ANOVA parameters

R- Squared	0.9911
Adj R-Squared	0.9798
Pred R-Squared	0.8908
Adeq Precision	22.260

- The "Pred R-Squared value" of 0.8908 is reasonable agreement with the "Adj R-Squared value" of 0.9798.
- "Adequate precision "value measure signal of noise ratio. It is desirable to have ratio greater than 4. Ratio of 22.260 indicates adequate signal. Hence model can be used.

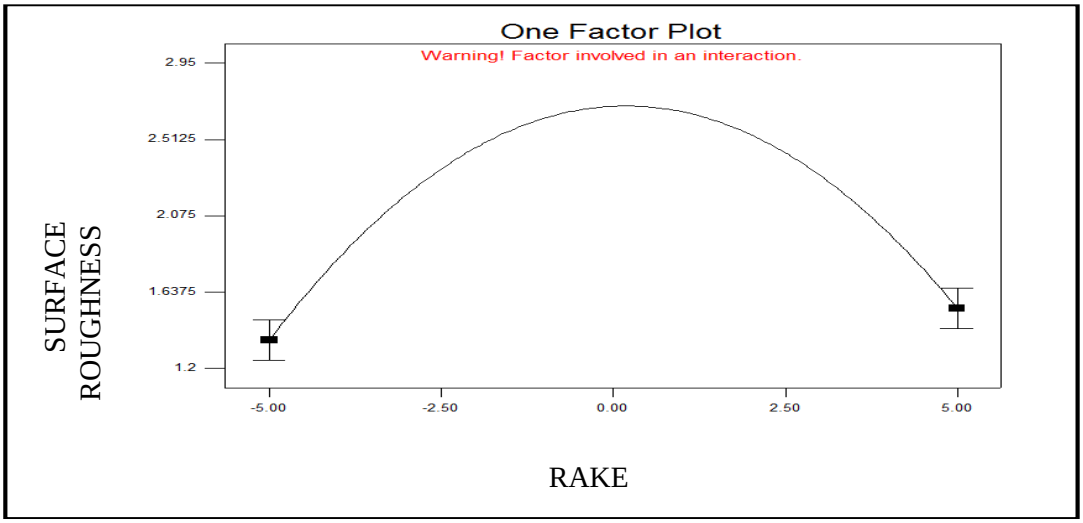

(a)

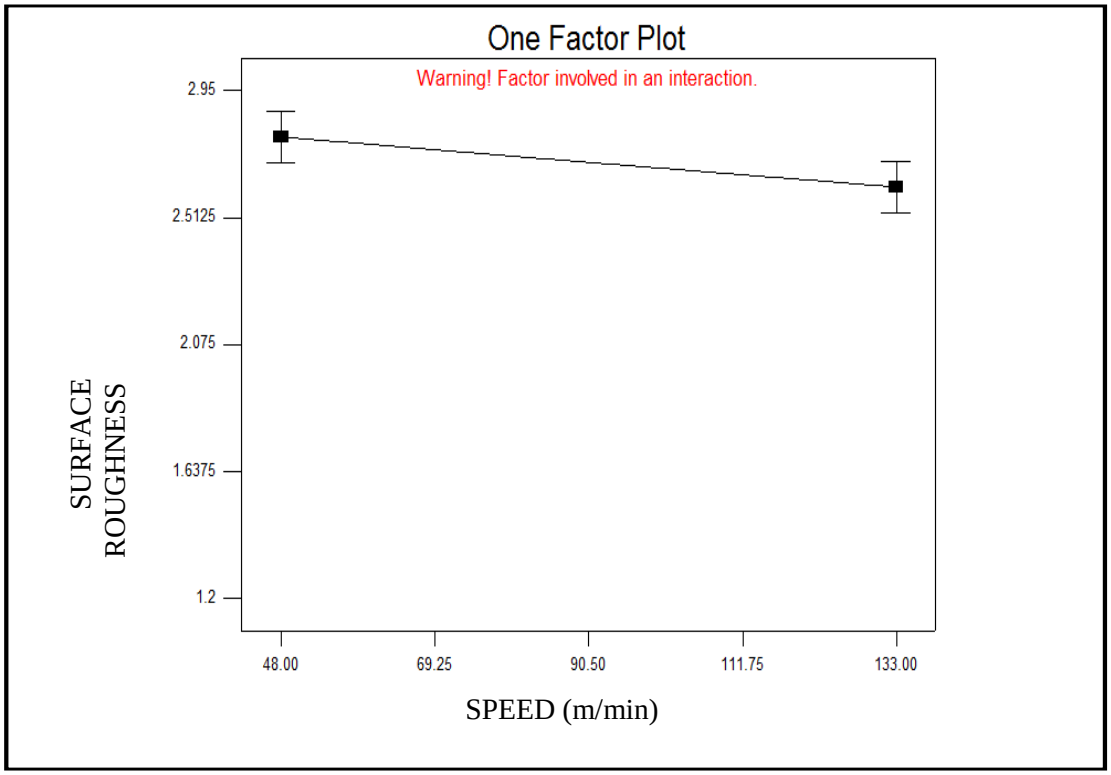

(b)

Figure 4.4 Variation of (a) Surface roughness v/s Rake (b) Surface roughness v/s Speed

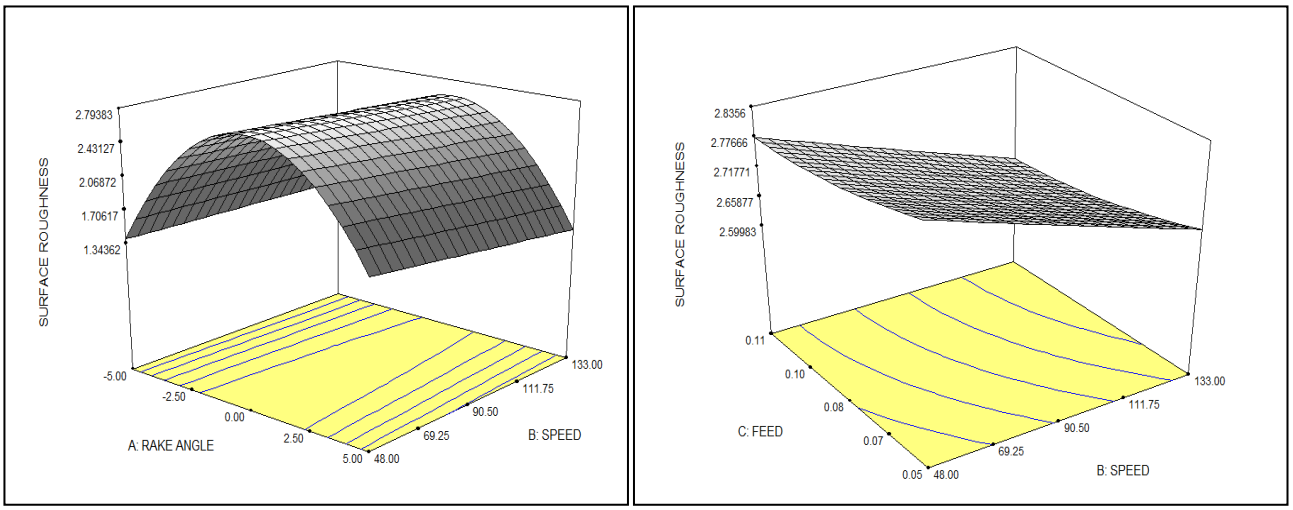

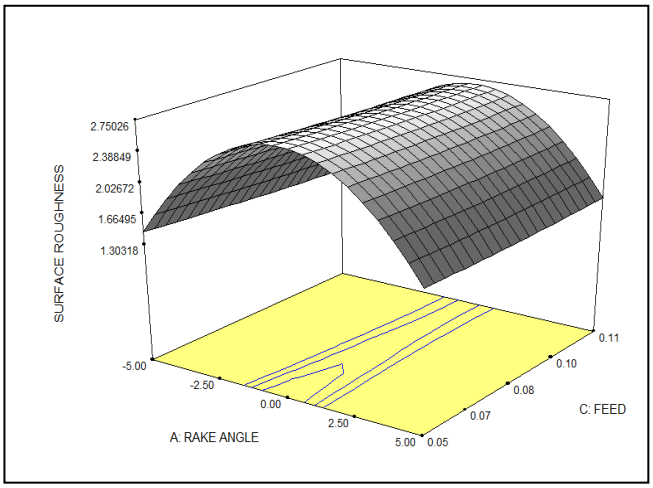

(c)

Figure 4.5 3-D plot of variation of (a) speed and rake v/s surface roughness, (b) speed and feed v/s surface roughness, (c) rake and feed v/s surface roughness

The dependency of surface roughness on cutting speed and rake angle is shown in figure 4.4and 4.5. Surface roughness of the samples decreases with increase in cutting speed and rake angle and with increase in feed surface roughness initially increases and then decreases. The reason being, with at low cutting speeds, matrix material is deformed to a lesser extent leading to discontinuous chip formation with cracks and higher surface

roughness. M.Prakash et al. [24] have studied the effect of cutting speed on surface roughness and a similar trend was observed in their investigation. Whereas with increasing rake angle, cutting forces and power consumption reduces causing less heat generation and tool wear which further promotes continuous chip flow with reduced surface roughness.

4.2.3 Analysis of SEM

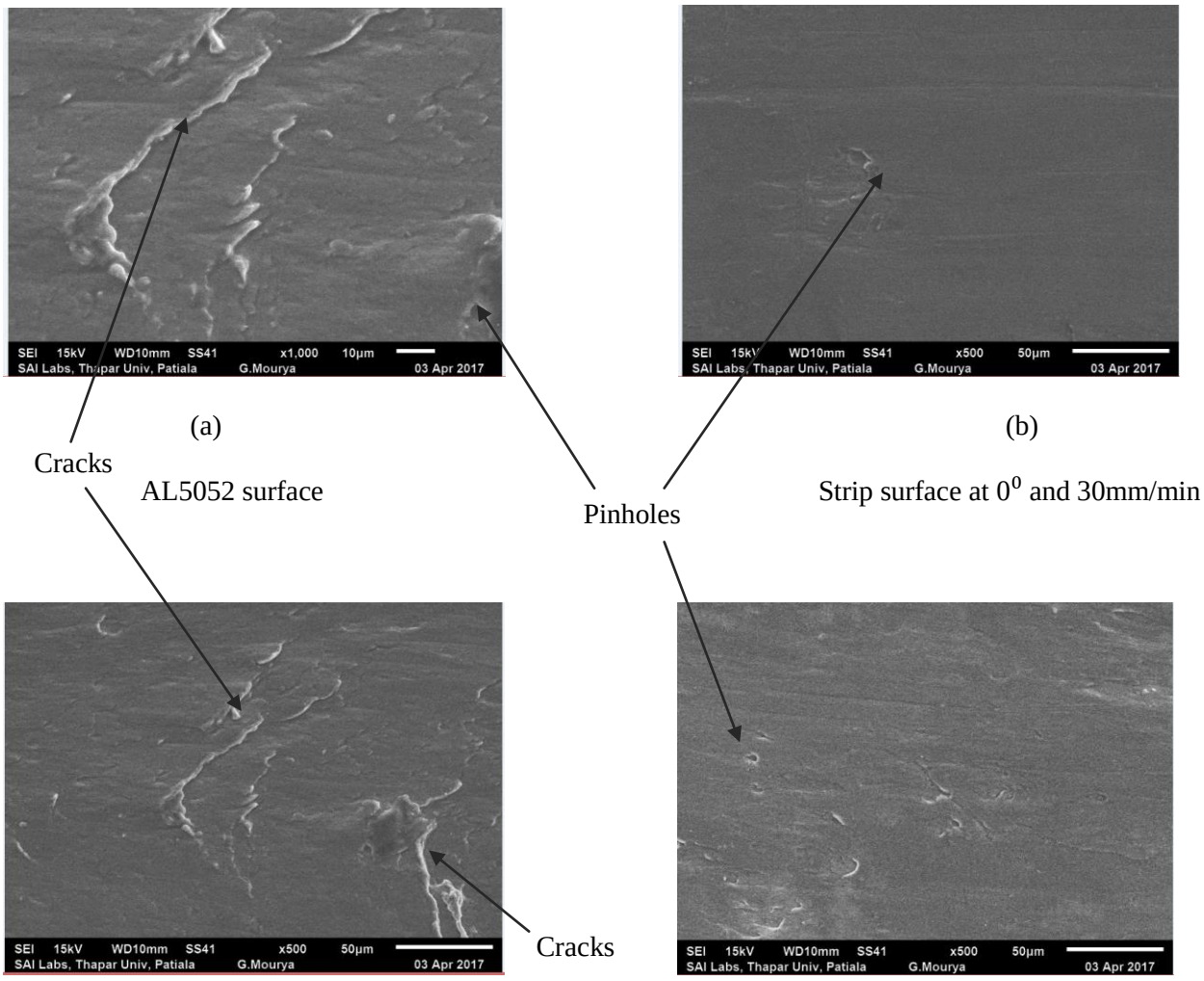

Figure 4.6 Surface of different strips

The surface morphology of chips produced by LSEM has been investigated by scanning electron microscope model JSM-6510LV. The SEM images were taken at 500x and 1000x resolution. The effect of feed and speed on surface quality of AL5052 chips produced by different rake angles have been shown in figure 4.6.It can be seen in 4.6(a) that surface of alloy AL5052 is very rough with asperities all over distributed uniformly. Strips produced by LSEM have fine surface as compared to alloy. It was found that strips with zero degree rake angle have finest surface of all followed by negative rake angle and positive rake angle simultaneously. It therefore follows the pattern shown above that surface roughness decreases with increase in rake angle.

4.2.4 Analysis of Shear Strain

In the Large strain extrusion Machining process severe plastic deformation is imposed on strips produced. In order to measure the level of deformation in strips, the shear deformation is carried out. Chip formation in machining occurs by concentrated shear in a narrow deformation zone, called the shear plane. In studies it was found that the shear strain increased with chip thickness ratio, it also increased with decrease in rake angle (α). The ability to control the position of constraint tool gives full flexibility to control strain in LSEM. The ability to control strain on the basis dual parameters rake angle (α) and chip thickness ratio (λ) in comparison to conventional machining where the shear strain is only depends on rake angle, the chip thickness cannot be predetermined. Thus it gives us an opportunity to study feasibility of LSEM as shear machining based deformation process. The mathematical relations of metal cutting process used to calculate chip thickness ratio (λ), shear strain (γ) and other parameters are described as follows. Chip thickness ratio (λ) can be expressed as

$$\lambda = \frac{tc}{t} \tag{4.3}$$

Where t_c = deformed chip thickness and t = undeformed chip thickness

The shear strain can be expressed as

$$\gamma = \frac{\lambda}{cos\alpha} + \frac{1}{\lambda cos\alpha} - 2tan\acute{\alpha} \tag{4.4}$$

Where α denotes tool rake angle, λ is the chip thickness ratio of the chip and γ is the shear strain.

Effective strain (E_{eff}) may be expressed as:

$$E_{eff} = \frac{\gamma}{\sqrt{3}} \tag{4.5}$$

Table 4.5 Table for shear strain

Rake angle	Speed	Feed	Λ	γ	E_{eff}
0	150	0.05	2.20	2.654	1.532
0	150	0.15	2.26	2.702	1.560
5	90	0.05	2.15	2.45	1.414
5	150	0.10	2.1	2.412	1.392
-5	30	0.10	1.92	2.623	1.514
-5	150	0.10	1.70	2.470	1.426
5	90	0.15	2.16	2.459	1.419
0	90	0.10	2.38	2.800	1.616
-5	90	0.05	1.85	2.573	1.486
0	90	0.10	2.41	2.824	1.630
0	30	0.15	2.52	2.916	1.683
0	90	0.10	2.38	2.800	1.616
0	90	0.10	2.32	2.751	1.591
-5	90	0.15	1.82	2.552	1.473
0	90	0.10	2.35	2.775	1.587
0	30	0.05	2.50	2.90	1.674
5	30	0.10	2.18	2.474	1.428

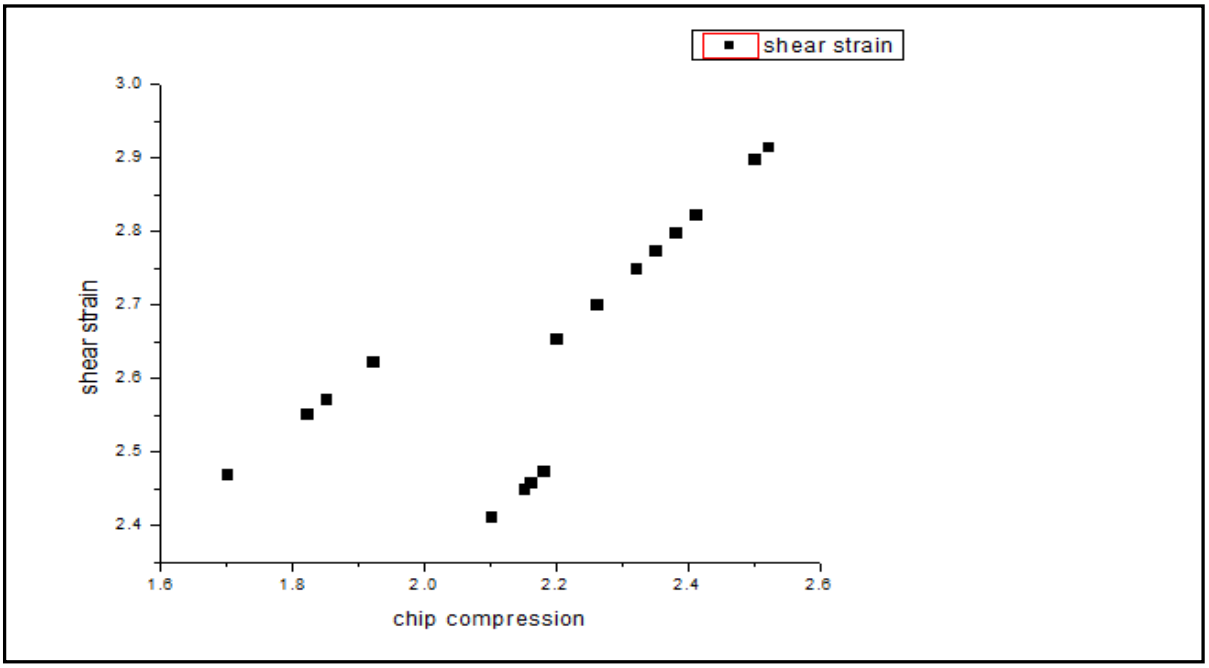

Figure 4.7 Variation between chip compression and shear strain

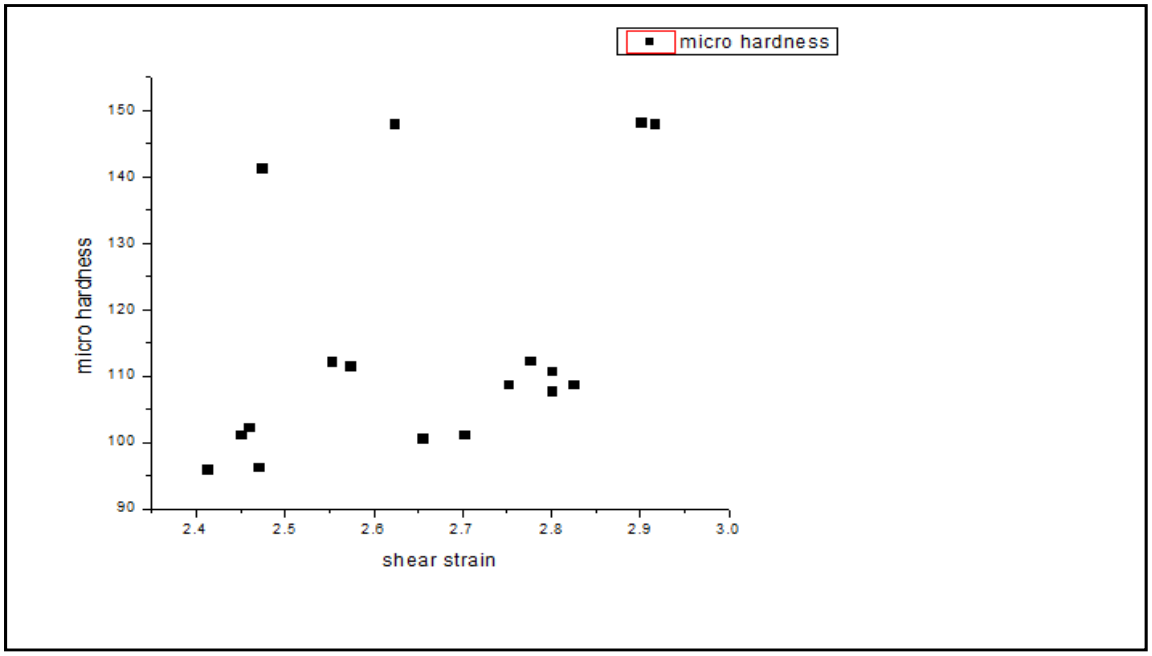

Figure 4.8 Variation between micro hardness and shear strain

The variation of γ with λ at three different rakes α = -5°, 0°, 5° and at three different cutting speeds v = 30 m/min, 150 m/min and 150 m/min and also at three different feeds 0.05 mm , 0.10 mm , 0.15 mm is illustrated . There is an increase in shear strain with increase in chip reduction coefficient. The shear strain also increases with decrease in rake angle .Due to less requirement of cutting forces and less frictional heating effect, energy required in deformation zone reduces as we increase rake angle [26].The deformation parameters are controlled by the constraint applied at point of chip formation by constraining. Thus this offers us a viable opportunity to study LSEM as a severe plastic deformation process.

4.2.5 Micro structural analysis using XRD

Crystallographic deformation was studied by XRD analysis. From the XRD patterns, six most intensive reflection peaks of the samples were used in the line broadening analysis. Table 4.6 shows the value of integral breadth and full width at high maximum (FWHM) value of the peaks at specific 2θ angle for all the machined samples and bulk aluminum.

Table 4.6 Crystallite size of Al-5052 samples investigated at different machining conditions using XRD technique

	Position 2θ(deg)	Height (counts)	FWHM 2θ(deg)	Area (counts*2θ)	Integral breadth(area/height) β_{exp}(degree)	Crystallite size (nm)
1.Bulk Aluminum						
1	33.7365	6578.8	0.2186	1438.12	0.218	132.16
2	42.0678	4320.21	0.0895	386.65	0.128	
3	65.3785	726.8	0.1404	102.04	0.140	
4	81.4086	1280.3	0.1786	228.66	0.178	
5	86.6825	700.85	0.0936	131.2	0.187	
6	103.2128	258.43	0.1872	96.76	0.374	
2.Aluminum strips made at -5°rake and V=30m/min						
1	33.7852	4881.3	0.2558	1847.87	0.378	58.4
2	42.0085	3562.85	0.1468	333.48	0.093	
3	65.3468	523.24	0.2303	178.27	0.340	
4	82.0089	1161.13	0.1092	253.59	0.218	
5	86.6877	439.57	0.307	199.68	0.454	
6	103.332	181.89	0.3744	136.2	0.748	
3.Aluminum strips made at -5° rake and V=90 m/min						
1	33.7808	6876.34	0.1919	1952.33	0.283	60.8
2	42.9759	4417.05	0.2175	1421.3	0.321	
3	65.6135	484.26	0.1092	105.76	0.218	
4	82.3265	1483.93	0.1716	509.28	0.343	
5	86.7288	459.41	0.1872	172	0.374	
6	103.0308	222.27	0.2808	124.83	0.561	
4.Aluminum strips made at -5°rake and V=150 m/min						
1	33.8792	4267.96	0.1716	1464.76	0.343	61.9
2	42.1455	4050.8	0.2808	2274.93	0.561	
3	65.4882	626.63	0.1404	175.96	0.280	
4	82.5832	1307.12	0.1092	285.47	0.218	
5	86.7706	461.08	0.2184	201.4	0.436	
6	103.3543	233.23	0.2184	101.87	0.436	

5.Aluminum strips made at 0°rake and V=30m/min						
1	33.7531	5979.52	0.2047	1810.88	0.302	61.48
2	42.0857	4226.74	0.2652	2241.86	0.530	
3	65.472	556.43	0.178	86.8	0.155	
4	82.5458	1447.12	0.1716	496.65	0.343	
5	86.7148	656.93	0.1092	143.47	0.218	
6	103.2943	228.91	0.1248	57.14	0.249	
6.Aluminum strips made at 0° rake and V=90m/min						
1	33.8455	4778.37	0.1768	542.67	0.113	68.82
2	42.0333	4750.66	0.1404	1333.98	0.280	
3	65.4079	722.77	0.1716	248.06	0.343	
4	82.6503	1500.09	0.156	468.03	0.312	
5	86.6967	366.14	0.1092	79.96	0.218	
6	103.2834	238.05	0.1936	44.56	0.187	
7.Aluminum strips made at 0°rake and V=150 m/min						
1	34.0356	3756.71	0.156	1172.09	0.311	71.8
2	42.3296	2919.97	0.1468	273.31	0.093	86.37
3	65.8605	472.69	0.178	73.74	0.156	
4	82.5724	975.5	0.1404	273.92	0.280	
5	86.8795	292.37	0.1092	63.85	0.218	
6	103.4871	191.78	0.1872	71.8	0.374	
8.Aluminum strips made at+5°rake and V=30m/min						
1	32.8196	5929.27	0.2175	1907.9	0.321	83.85
2	42.1316	3249.41	0.156	1013.82	0.312	
3	65.4943	658.3	0.1092	143.77	0.218	
4	82.8089	1026.12	0.2496	512.24	0.499	
5	86.6784	494.46	0.1092	107.99	0.218	
6	103.3545	149.61	0.1248	37.34	0.249	
9.Aluminum strips made at +5°rake and V=90 m/min						
1	33.8237	7898.06	0.1791	2092.92	0.264	84.2
2	42.9987	5028.23	0.2047	1522.79	0.302	
3	65.4241	764.16	0.1716	262.26	0.343	

4	82.4801	1351.44	0.1404	379.48	0.280	
5	86.7233	606.86	0.1404	170.4	0.280	
6	103.2764	244.37	0.0936	45.75	0.187	
10.Aluminum strips made at +5°rake and V= 150 m/min						
1	33.8456	8540.84	0.2047	2586.58	0.302	86.8
2	42.0789	5349.99	0.0895	708.85	0.13	
3	65.4026	686.8	0.1404	192.85	0.280	
4	82.5736	1416.43	0.1872	530.31	0.374	
5	86.7526	700.85	0.0936	131.2	0.187	
6	103.3526	258.43	0.1872	96.76	0.374	

From Fig 4.9 illustrates a combined comparative layout of different Bragg's peaks of XRD pattern and it can be clearly observed the presence of a single phase and no change in phase due to SPD of the machined samples.

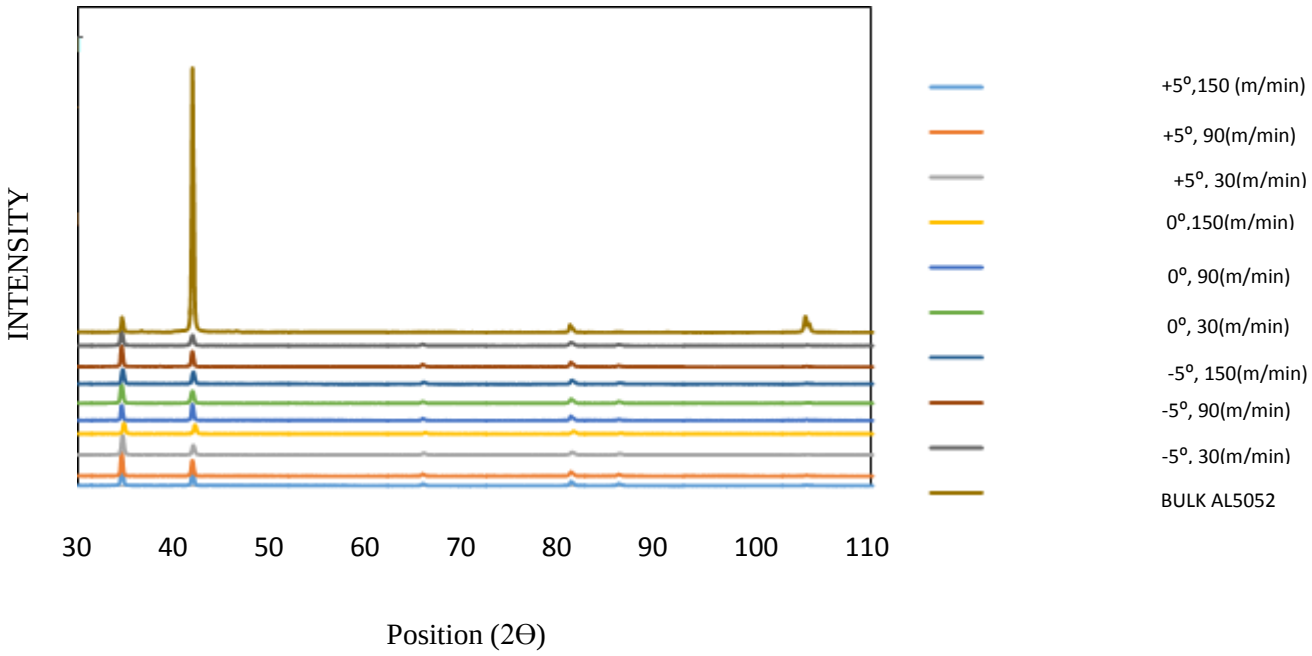

Figure 4.9 Combined graph of Bragg's peaks of XRD pattern for bulk and different machining conditions

It can be seen that as the rake angle and cutting velocity decreases the peaks of XRD are found to be broaden. This broadening of XRD peaks with corresponding decrease in peak height illuminates the effect of severe plastic deformation (SPD).With XRD peaks broadening, the increasing intensity of SPD can be observed, which marks decreasing crystallite size.[27]

CONCLUSIONS

On the basis of the conducted work on LSEM for fabrication of AL5052 aluminium alloy strips and different characterization performed to evaluate mechanical and micro structural properties, the following conclusions can be drawn,

- The shear strain was found to increase with decrease in rake angle for different strips, similarly shear strain with increased with increase in chip thickness ratio.
- Both cutting speed and cutting tool rake angle play a major role while feed play a minor role in controlling the strain and dimensional tolerance of the strips.
- At higher feed surface roughness is found to be high.
- Micro hardness was found to be increased with cutting speed and decreased with rake angle while the feed has least effect on micro hardness.
- The micro hardness of produced strips approximately was 40%-60% higher than the AL5052 alloy.
- The surface quality of strips improves with increase in rake angle and cutting speed.
- Surface morphology is found to be directly dependent on rake angle.
- From XRD analysis, crystallite size was found to be decreasing with increasing strain.
- Surface roughness of the fabricated strips was found to be improved by an average of 20% with increasing cutting velocity and rake angle.

REFERENCES

[1] Sung H. Whang, Nanostructured metals and alloys- Processing, microstructure, mechanical properties and applications, *Fundamentals of aluminum metallurgy*; ISBN 978-1-84569-654.

[2] SrinivasanSwaminathan, M. Ravi Shankar, Seongyl Lee, Jihong Hwang, Alexander H. King, Renae F. Kezar, Balkrishna C. Rao, Travis L. Brown, SrinivasanChandrasekar, W. Dale Compton, Kevin P. Trumble. Large strain deformation and ultra-fine grained materials by machining Materials, *Science and Engineering A*2005; 410–411:358–363.

[3] A. E. Giannakopoulos and S.Suresh.,Determination of elastoplastic properties by instrumented sharp indentation,*ScriptaMaterialia*1999(10); 40:1191–1198.

[4] P. Iglesias, M.D. Bermúdez, W. Moscoso, S. Chandrasekar. Influence of processing parameters on wear resistance of nanostructured OFHC copper manufactured by large strain extrusion machining, *Wear* 2010; 268:178–184.

[5] Travis L. Brown, Christopher Saldana, Tejas G. Murthy, James B. Mann, Yang Guo, Larry F. Allard, Alexander H. King, W. Dale Compton, Kevin P. Trumble, SrinivasanChandrasekar. A study of the interactive effects of strain, strain rate and temperature in severe plastic deformation of copper, *ActaMaterialia* 2009; 57:5491–5500.

[6] M. Sevier, H.T.Y. Yang, W. Moscoso, and S. Chandrasekar. Analysis of Severe Plastic Deformation by Large Strain Extrusion Machining, *Metallurgical and materials transactions A* 2008; 39:2645-2655.

[7] L. De Chiffre. Extrusion cutting of brass strips, *International Journal of Machine Tool Design and Research* 1983; 23:141-151.

[8] Wen Jun Deng, Ping Lin, Zi Chun Xie, and Qing Li. Analysis of large-strain extrusion machining with different chip compression ratios, *Journal of Nanomaterials* 2012.

[9] Wen Jun Deng, Ping Lin, Qing Li & Wei Xia. Effect of Constraining Tool Corner Radius on Large Strain Extrusion Machining, *Materials and Manufacturing Processes* 2013; 28:1090-1094.

[10] Wen Jun Deng, Yong Tai He, Ping Lin, Wei Xia & Yong Tang. Investigation of the Effect of Rake Angle on Large Strain Extrusion Machining, *Materials and Manufacturing Processes* 2014; 29:621-626.

[11] S.L. Cai, Y. Chen, G.G. Ye, M.Q. Jiang, H.Y. Wang, L.H. Dai(2015), Characterization of the deformation field in large-strain extrusion machining, *Journal of Materials Processing Technology*, 216:48-58.

[12] W. Moscoso, M.R. Shankar, J.B. Mann, W.D. Compton, S. Chandrasekar, Bulk nanostructured materials by large strain extrusion machining, *Journal of Materials Research* 2007; 22:201-205.

[13] Ping Lin, Zin Chum XieabdQuig Li, Efeect of friction coefficient on large strain extrusion machining, *Journal of Applied Mechanics and Materials*,2013;273:138-142.

[14] P. Iglesias, M.D. Bermudez, W. Moscoso and S. Chandrasekar ,influence of processing parameters on wear resistance of nanostructured OHFC copper manufactured by large strain extrusion machining,Journal of Wear ,2010;268(1):178-184.

[15] Travis Brown, L.Saladana, Christopher Murthy , Tejas G. Mann, James B Guo,Larry F King ,W.D.Trumble, S. Chandrasekhar, A study of interactive effect of strain,strain rate and temperature in severe plastic deformation of copper , ActaMaterialia ,2009;57:5491-5500 .

[16] MertEfe, WilfredoMoscoso, Kevin P. Trumble, W. Dale Compton, SrinivasanChandrasekar. Mechanics of large strain extrusion machining and application to deformation processing of magnesium alloys, *ActaMaterialia* 2012; 60: 2031–2042.

[17] Andrew Kustas, Kevin Chaput, SrinivasanChandrasekar, Kevin Trumble. Quality of strips produced by extrusion machining directly from Cast 5052 Aluminum, *Material science and technology* 2014; 79-86.

[18] M.Ravishankar, B.C. Rao, S. SrinivasanChandrasekhar,W. Dale Compton, Alexander H. King ,Thermally stable nanostructured materials from severe plastic deformation of precipitation-treatable Ni-based alloys, *Journal of material science*,2005;158:70-75.

[19] W.J. Deng, Q. Li, B. Li, Z.C. Xie, Y.T. He, Y. Tang, Thermal Stability of ultrafine grained aluminium alloy prepared by Large Strain Extrusion machining, *Journal of material science and technology*,2014;30:850-859.

[20] DinakarSagapuram, MertEfe, WilfredoMoscoso, SrinivasanChandrasekar, Kevin P. Trumble, Deformation Temperature Effects on Microstructure and Texture Evolution in High Strain Rate Extrusion-Machining of Mg-AZ31B, *Journal of Materials Science* 2012; 702-703:52-55.

[21] P. Iglesias, W. Moscoso, J.B. Mann, C. Saldana, M. R. Shankar, S. Chandrasekar, W. D. Compton and K. P. Trumble. Production analysis of new machining-based deformation processes for nanostructured materials. *International Journal of material forming*,2008; 1:459–462.

[22] Y. Guo,M. Efe,W. Moscoso,D. Sagapuram,K.P. Trumbleand S. Chandrasekar. Deformation field in large-strain extrusion machining and implications for deformation processing *ScriptaMaterialia* 2012; 66:235–238.

[23] http://ksm.fsv.cvut.cz/~nemecek/teaching/dmpo/Nemecek_nanoindentation.pdf.

[24] M.Prakash,S.Shekhar,A.P.Moon,K.Mondal. Effect of machining configuration on the corrosion of mild steel, *JournalofMaterialsProcessingTechnology*2015; 219:70–83.

[25] Ravinder Singh Joshi, SidhantSrivastava, Harpreet Singh. Microstructural analysis of nanostructured aluminum alloy strips created from machining based deformation process, 6th CIRP International Conference on High Performance Cutting, HPC2014.

[26] Tensile Testing, 2nd edition. Joseph R. Davis, ASM Publisher 2014; ISBN 1615030956, 9891615030958.

[27] Travis Brown, Christopher Murthy , Tejas G. Mann, James B Guo, Larry F King, Srinivasan Chandrasekhar, A study of interactive effect of strain,strain rate and temperature in severe plastic deformation of copper, ActaMaterialia,2009;57:5491-5500 .